Article:
Fantham, T.L. and Gladwin, D.T. orcid.org/0000-0001-7195-5435 (2022) Enabling accurate and fast large-scale battery simulation using only a 9-cell model with variance based parameters. Journal of Energy Storage, 54. 105225. ISSN: 2352-152X

https://doi.org/10.1016/j.est.2022.105225

Journal of Energy Storage 54 (2022) 105225

Contents lists available at ScienceDirect

Journal of Energy Storage

journal homepage: www.elsevier.com/locate/est

Research papers

Enabling accurate and fast large-scale battery simulation using only a 9-cell model with variance based parameters

T.L. Fantham, D.T. Gladwin *

Centre for Research into Electrical Energy Storage & Applications, Department of Electronic and Electrical Engineering, The University of Sheffield, Sir Frederick Mappin Building, Mappin Street, Sheffield S1 3JD, UK

ARTICLE INFO

Keywords:
BESS model
Grid-scale storage
Electric vehicle battery
Lithium-ion battery
Cell balance
Battery parameter identification

ABSTRACT

For grid-connected batteries consisting of upwards of tens of thousands of cells, it can be challenging to produce an effective electrical model. Two methods are commonly seen in literature to model large packs, either represent the pack with a single cell model, or represent the pack with a cell model for every cell. The former is computationally efficient and suitable for real-time applications but lacks individual cell-level behaviour across the pack, whilst the latter offers this, due to the model size, it is unsuitable for real-time applications. Thus, a novel model is presented that can represent any size of battery pack using up to nine cell-models. A method for identifying the parameters for the nine cell models is offered, focused on ensuring the capacity limiting "weakest cell" is accounted for. This is verified experimentally with two lab-scale tests and a method for identifying parameters for a large sample of cells using the parameter distribution is evaluated. For a 48 cell pack under 1C charge/discharge cycles, modelling all cells was identical to the proposed model, with an accuracy of >99.4 % compared to experimental testing whilst being >20 times faster to simulate. The simulation time for the proposed model to provide 10 real-time hours of data was 3.7 s, compared to modelling all 48 cells in the pack requiring 79.6 s. Finally, using the parameter distribution or variance is shown to be a viable technique to estimate the achievable pack capacity, with a 1C cycle test experimentally achieving an accuracy of >98.9 % when identifying model parameters using the variance of a sample of cells.

1. Introduction

Large battery packs are increasingly becoming more common, with applications vastly growing as the need for electricity storage is increasing. This can include electric vehicles where there may be hundreds to thousands of cells in a car [1,2] and upwards of tens of thousands in a large grid-connected battery energy storage system (BESS) [3]. These can be even larger when using smaller cells in these large packs, such as the cylindrical 2170 cell which is used in the Hornsdale Power Reserve - a 100 MW/129MWh BESS built by Tesla [4,5].

Previous work presented in [6] introduced how cells connected in a pack are not identical, and that this can affect the performance of the overall pack. For a series string, it was shown that the overall capacity of a pack is generally limited by a single "weak" cell. This paper explores creating an accurate yet computationally efficient model which takes into account this behaviour, combining different approaches.

When performing analysis on a multi-cell pack, such as real-time state estimation or simulation, two main approaches are used when modelling the pack. The first is to model every cell individually, as represented by Fig. 1, and discussed in [7–9]. This would give the most complete picture of the state of the battery, with an estimate for every single cell in the pack to give the best understanding of the overall pack performance. However, it is challenging to monitor, store, and process data from every cell in a pack. As an example, the Willenhall Energy Storage System (WESS), a 1 MW, 2MWh battery system operated by the University of Sheffield (see [3] for more details), contains 21,120 cells. There are typically 2 bytes per data frame for each cell containing voltage readings which are reported by the cell management system to the battery management system every 120 ms. This is 21.1 KB of data per 120 ms and therefore 176 KB/s. Over a single day, stored with no compression, this would produce 15.2GB of data. Whilst not impossible to deal with, processing all data in real time for every cell in the pack could pose a challenge due to the large processing requirements. Various solutions have been proposed and implemented in different systems, including pre-processing in each battery module and reporting back information such as State-of-Charge (SoC) and State-of-Health (SoH) for

* Corresponding author.
E-mail addresses: tfantham1@sheffield.ac.uk (T.L. Fantham), d.gladwin@sheffield.ac.uk (D.T. Gladwin).

https://doi.org/10.1016/j.est.2022.105225
Received 11 April 2022; Received in revised form 8 June 2022; Accepted 25 June 2022
Available online 26 July 2022

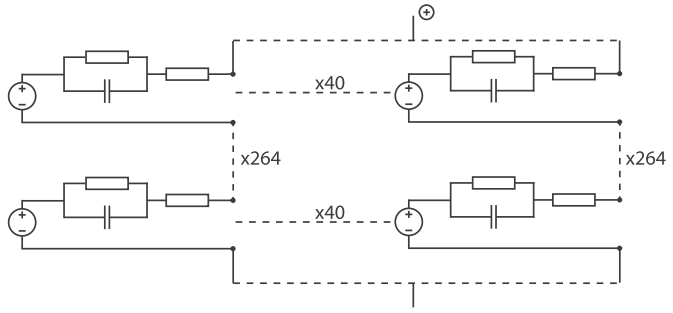

Fig. 1. A model representation of WESS showing every cell being modelled, with each string containing 264 parallel pairs of 2.7 V (max), 20 Ah cells. There are 40 strings connected in parallel.

each cell, rather than just voltage data [10]. Even with the processed information for each cell, this will still not be able to give a complete picture of the overall output performance of the battery - the state of charge or the overall available energy capacity at the terminals. This would again mean further processing to give this information.

The same issues are faced in the simulation of large-scale packs. As an example, modelling a single cell with a zero-order Equivalent Circuit model (Rint Model, as described in [11,12]) in Simulink as detailed in Section 2.1, takes 1.7 s to perform a single cycle (charge and discharge) at 1C with a 1 s sample rate on a modern computer (CPU - i7 7700, 24GB RAM, SSD). A number of simulations were performed with different pack configurations for 7200 s simulation time and the results can be seen in Fig. 2 which shows how the real processing time varies with the number of cells being simulated.

Interpolating Fig. 2 for WESSs 21,120 cells, it can be estimated that simulating WESS for a simulation time of 7200 s would take approximately 7500 s of processing on a modern computer (specification mentioned previously). With the processing time being longer than the simulation time, it makes the approach unsuitable for real-time applications and time consuming for general simulation, though the ever advancement of computing power may see this approach more feasible in the future.

The second approach is to model the entire pack as a single cell model such as those seen in [13,14], shown in Fig. 3. It can be effective as it is fast and straightforward to implement and allows the use of a more computationally intensive cell model as only a single cell is simulated. However, the main issue with this is the loss of accuracy in

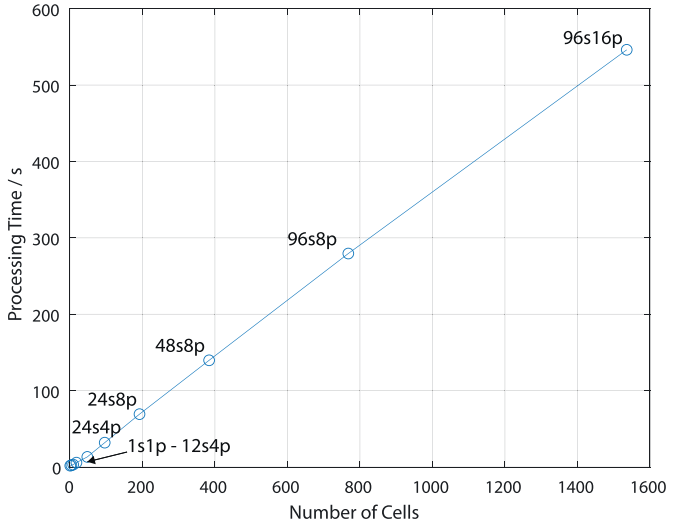

Fig. 2. Processing time vs number of cells for a Rint model for various pack configurations.

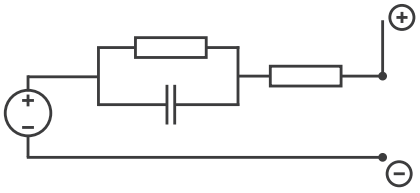

Fig. 3. A single cell model representation of WESS showing just a single cell being modelled, totalling the voltage and capacity of the model shown in Fig. 1.

the model due to the cells in the pack not being identical. In other words, at any given time, the cells will not necessarily all have the same voltage and current flow due to differences in capacity, impedance, and other parameters. For a practical system, it is expected that modelling the pack with a single cell model would result in the system reporting a larger amount of energy available than is actually available, due to some cells reaching their voltage limits before others meaning some cells have unreachable capacity. This would vary depending on how well balanced the system is at any given time.

In reality, the only important readings are the lowest and highest cell voltage as a full charge/discharge cycle must end or change when one cell reaches its upper or lower voltage limit. The work in [6] has shown that this will always take the place of a single cell which can be considered the “weakest cell”. The weakest cell in a series string will reach its voltage limit before all others, assuming the string is balanced. A string or pack is considered balanced if the SoCs of all cells becomes equal at any point during a cycle. A Battery Management System (BMS) will typically manage the balance state of a pack, using a cell balancing mechanism. These mechanisms are split into two categories, passive and active [15]. A passive BMS consists of switched resistors which discharge higher voltage cells to balance a pack, normally whilst the pack is at rest and when almost fully charged. An active BMS consists of controlled electronic switches that enables the transfer of charge between cells. An appropriate active BMS is an alternative approach to the improved modelling presented in this paper, albeit at an increased cost, as it can help avoid limitations of the weakest cell by transferring charge from the strongest to the weakest cell.

The approach proposed in this paper aims to improve on battery pack models, by producing a model with a sufficient view of the state of the cells within the system, without having to model every single cell. The approach revolves around the concept that it's only necessary to know the maximum and minimum cell voltages to predict the remaining charge that can be put into the battery and removed from the battery. One method is to model the single weakest cell (the cell with the lowest capacity and highest impedance) alongside the model representing the whole pack. This results in the model consisting of just two cell models.

This should show an improvement in the accuracy, but the model lacks the data for currents inside the system (such as between parallel strings), so assumes that there is equal current between strings in the system. Furthermore, it cannot give a measure of cell voltage imbalance - the difference between the highest and lowest cell voltages. Many systems operate with cell voltage imbalance as a limit to prevent large currents between parallel strings. These two metrics (cell voltage imbalance and maximum string current) should therefore be output from the model.

To give a value for cell voltage imbalance for a series string, it is proposed that 3 cell models are required. The strongest cell, the weakest cell, and the remaining cells as a single cell model, shown later in Fig. 13. This study defines the weakest cell as the cell which reaches the upper/lower voltage limits under charge/discharge and the strongest cell is defined as the cell which remains furthest from the voltage limits, assuming the pack is balanced at a given SoC (i.e. the cell voltages converge at a the given SoC). This will give the highest, lowest, and average cell voltage, as well as the SoC of each cell model and therefore the overall SoC. Current is constant between cells in the string.

To give a value for the maximum current between any number of cells connected in parallel, it is proposed that 3 cell models are required. Again, the strongest, weakest, and remaining cells, shown later in Fig. 15. As the voltage is constant in the parallel connections, the current between the cells can be calculated. It is expected that this will give the maximum current, as there will be the highest current through either the strongest or weakest cell.

From this, to model a pack of any size with any combination of parallel and series connections, at most nine cell models are required as a combination of the series and parallel models, which is the final model proposed in this paper, represented in Fig. 4. With improved pack accuracy, and reduced computation, this would allow the use of a more complex cell model in a pack, such as that seen in [16].

The main contributions of this paper are listed as follows.

1. A 9 cell model is presented that can be used to simulate large battery packs and 20 times.
2. A method for identifying the parameters for the model is proposed and demonstrated.
3. The model and identification method is verified experimentally with a 12s4p pack with >99 % accuracy for capacity estimation.
4. The simulation speed is shown to be >20 times faster than when modelling all cells in the pack.
5. It is demonstrated experimentally how parameters can additionally be identified using cell variance data.

The remainder of the paper is organised as follows. Section 2 describes the model proposed in this paper, detailing the cell model and following scale up to pack model. Section 3 details the parameter identification procedure, showing experimental results to highlight the variance between cells. An evaluation of the model is presented in Section 4, with experimental results from a 12s4p pack providing grounding in reality. Finally, the conclusions are presented in Section 5.

2. Modelling

The proposed model containing 9 cells to make up the overall pack model is produced using Simulink named the 9 Cells Model (9CM). This section will discuss the architecture of the model, beginning with the individual cell model, discussing the input parameters, and justifying the details of the model. It will then be shown how the 9CM is scaled from single cell models.

2.1. Cell model

The cell model used is an Equivalent Circuit Model - these represent the cell as an electrical circuit, typically consisting of a voltage source, which varies based on SoC, and additional components to represent the impedance. In this paper, the model was built in Simulink, functioning as a Rint model, as shown in Fig. 5 where the internal resistance varies with the current direction (charge or discharge) (seen in [7,17]) and the temperature. Additionally, the capacity degrades on cycling [11,12]. One negative aspect of the Rint model is that it will not correctly show the dynamic behaviour of the pack, meaning that during a large change in current, the voltage shown by the model may not exactly match experimental values due to the transient behaviour of the battery. The Rint model was however chosen for several reasons. Firstly, in a grid-scale system, the largest concern is about reaching the voltage limits. The Rint model will show the 'worst case scenario' where the steady-state behaviour will be reached immediately. Next, the study is looking more closely at the variations between large numbers of cells. It is relatively straightforward to identify the parameters for the Rint model, meaning a large dataset can be used to give the variance of a group of cells without the need for impedance measurements at a range of frequencies on individual cells. Finally, this study is more concerned with the process of modelling a large number of cells, rather than producing an unnecessarily complex cell model. The parameters that are considered are those that are most relevant to a grid scale system, however, it would be possible to increase the order of the model if the results show that a Rint model is insufficient. Fig. 6 shows the design of the cell model in Simulink.

2.1.1. Model parameters

The physical parameters which are used in the model include:

1. Capacity
2. OCV

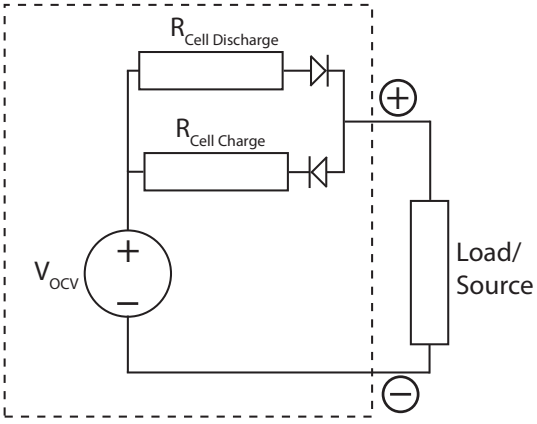

Fig. 5. The proposed Rint cell model.

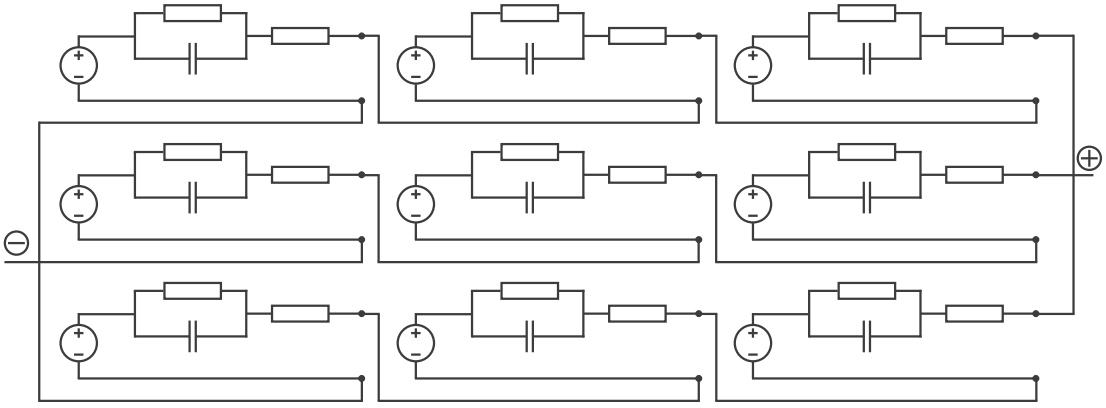

Fig. 4. Configuration of the 9 cells model proposed in this paper.

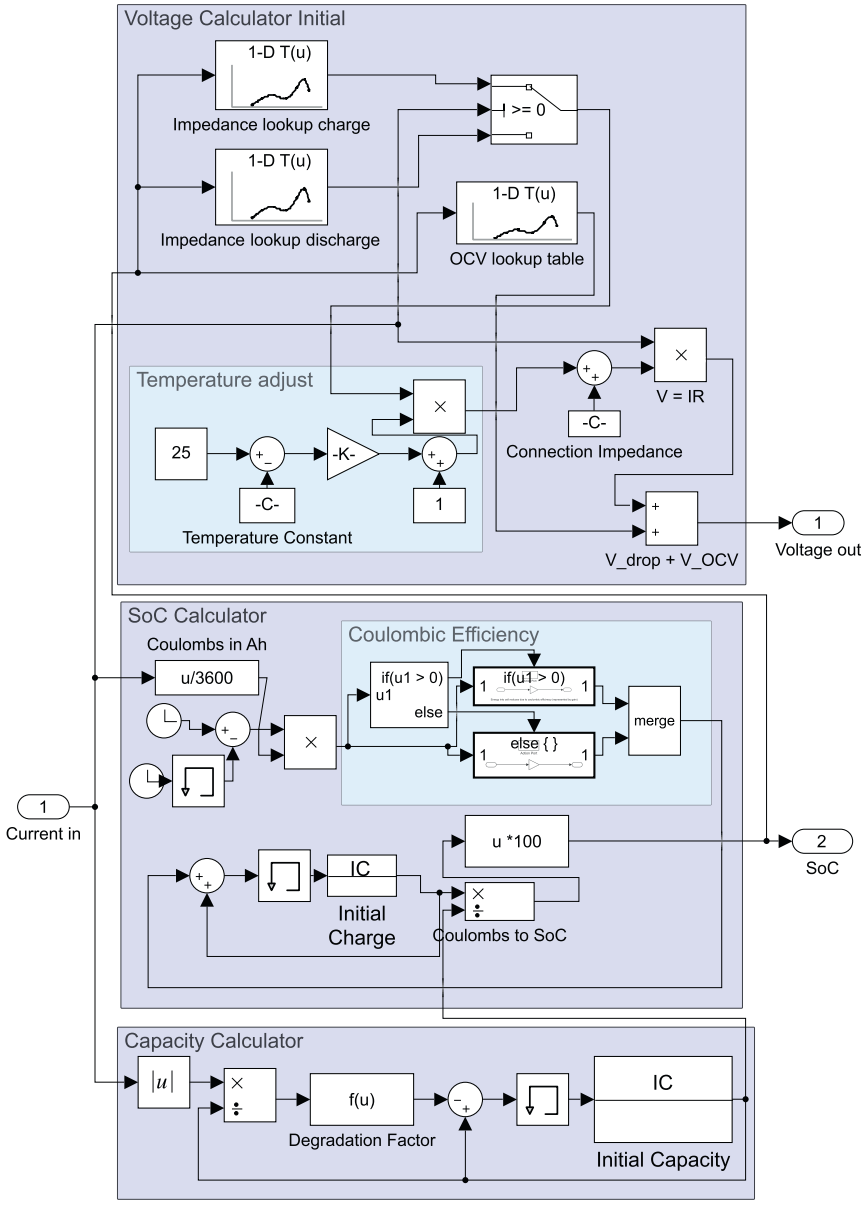

Fig. 6. Implementation of the Rint model in Simulink.

3. Impedance
4. Temperature
5. Coulombic efficiency
6. Degradation rate.

Each of these parameters has been considered individually and experimentally verified to determine how they are implemented in the cell model. This section describes the chosen implementations for each parameter.

For experimental validation, a sample of ten Yuasa LIM5H cells were used. Ten were used to give nine cells to identify the parameters for the 9CM and a spare. They were chosen as they are of a lithium-NMC type chemistry - a widely used cell chemistry [18].

2.1.1.1. Capacity. . The capacity of a cell describes the Coulombic charge which can be extracted from or input to it, before voltage limits are reached. The capacity of a cell is measured using a Constant Current, Constant Voltage (CCCV) charge/discharge test to determine the maximum capacity of a cell, using the procedure shown in Table 1. Using a CCCV discharge to measure capacity is atypical, but is used in this case as the capacity must represent the full Coulombic charge stored in the battery.

Table 1
Test procedure for measuring capacity of cells.

	Step	Sequence	Limits	End Conditions
Capacity Test	1	CCCV Charge	V ≥ Max V, I = 1C	I < C/20 A
	2	CCCV Discharge	V ≤ Min V, I = 1C	I < C/20 A
	3	CCCV Charge	V ≥ Max V, I = 1C	I < C/20 A

The CV cutoff current used is C/20, a value commonly used in literature [19,20]. This is an important choice as a model would consider the battery to have reached 100 % or 0 % SoC once a CV charge or discharge has reached C/20, even though more energy could be charged or discharged at lower C-rates. In the literature, C/20 appears to be a suitable balance between having a good measurement for capacity and not having an unnecessarily lengthy test time.

2.1.1.2. OCV. . Open-Circuit Voltage (OCV) refers to how the voltage of a battery at rest (i.e., no current flow and the voltage is unchanging) changes depending on the charge in the battery. It is highlighted in [11,12] the importance of good Open Circuit Voltage (OCV) measurement for having a good SoC estimate.

It is important to understand how the OCV changes depending upon the state of charge. When using a Randles model, OCV is the key in determining the voltage at any point, with the voltage deviating from OCV on the application of current and subsequent voltage drop [22].

The datasheet for any particular cell generally states OCV, however it is useful to perform a test to verify this. This involves discharging in 10 % increments of SoC, followed by charging in the same increments as shown in Fig. 7.

The test begins with a full 1C cycle to ensure consistent behaviour (not shown in Fig. 7) before performing the OCV test. The capacity test is performed immediately before the OCV test, as the capacity is needed to perform the OCV test. Once the capacity of the pack is known, the pack is discharged and then charged in 10 % capacity increments at 1C, with a CV discharge at the end of the last discharge pulse to ensure the cell is at 0 % before beginning the first charge pulse - a method seen used in literature [23]. There is a 2 h rest between each pulse and the average voltage between the charge and discharge for SoC is taken to eliminate any hysteresis or to compensate for where the cell has not completely reached a constant resting voltage - the latter typically occurs at a low SoC as seen in Fig. 7.

Considering SoC accuracy for each pulse point for the OCV test shown in Fig. 7, the discharge capacity measured during the capacity test was 5.256 Ah and the total capacity discharged during the pulse discharges totalled 5.274 Ah. This is a 0.3 % difference meaning each OCV measurement is within at least that margin of error in terms of SoC.

2.1.1.3. Impedance. . Impedance in a cell causes a voltage drop due to the current through it. In the Rint model, the voltage is dropped across the series resistance, seen previously in Fig. 5.

The voltage drop can be found as $V_{drop} = IR$ and the impedance (R) can therefore be found through a known change in current and measuring the subsequent change in voltage as per Eq. (1) as described in [12].

$$R_{DCIR} = \frac{\Delta V}{\Delta I} \tag{1}$$

Whilst straightforward, this presents issues in measurement. Immediately measuring the voltage after a current change will result in a low value for R_{DCIR} due to the transient behaviour. Measuring the voltage after a longer period of time after a current change to a nonzero current would result in a change in SoC and therefore give a larger R_{DCIR} reading. Therefore, a suitable way to calculate R is to measure the voltage once it has reached steady-state and change the current from a specified value to zero to eliminate a change in SoC [20]. The decision then lies on how long a rest period is required to reach the end of the transient behaviour, where the voltage returns to the OCV.

Fig. 8 shows that measuring for different lengths of time results in a different measurement for impedance. A very short test (<1 s) provides the value known as R_0 - or the purely ohmic component of a multi-order Randles model [20]. A much longer test, in the shown case upwards of 1 h, shows the charge transfer resistance [24] (R_{CT}) (the resistance due to charge transfer at the interface between the electrode and electrolyte) and the polarisation resistance [17] (R_p) (the resistance due to ionic diffusion). Inductive impedance is dominant at time periods shorter than 1 ms, though ramp current ramp rates ($\frac{di}{dt}$) and inductance small enough such that it is insignificant to the measurable time domain response. As an example, inductance for a cell is in the order of 10^{-8}H, and the MACCOR S4000 cell tester ramps to its maximum current (10A) in 500 μs. This would give a ΔV of 0.2 mV, which is less than the 0.3 mV resolution for a time period shorter than the 10 ms fastest sample rate. Hence, the inductive impedance is ignored going forwards. Therefore R for the Rint model is shown as per Eq. (2):

$$R_{DCIR} = R_0 + R_{CT} + R_P \tag{2}$$

The transient behaviour of these cells ends after 2 h at most SoCs, so 2 h will therefore be used as the rest time for subsequent impedance experiments using these cells. However, this is only necessary to calculate the open-circuit voltage. If coulomb-counting can be used to estimate the state-of-charge, then the open circuit voltage can be used instead of waiting for 2 h. This can vastly accelerate the testing procedure. Therefore, instead of $\Delta V = V_{load} - V_{rest}$ to find the voltage drop, $\Delta V = V_{load} - V_{OCV}$ can be used.

Naturally, a lengthy OCV test is still required on at least one cell, as well as high-precision current sensing to provide suitably accurate coulomb-counting to give a good estimate for SoC. It should also be the most accurate method, as in the model, the voltage is estimated based upon the OCV and the voltage drop caused by the impedance under load. For identifying parameters using this method, the impedance is calculated based upon the estimated OCV, the measured voltage under load and the measured current. This is essentially a direct inverse as the OCV-SoC relationship is the same in the model and the parameter identification.

All measured values assume that all resistance is from the cell, and not from any physical connections. This is justified as the tests use remote voltage sense, and due to the very low current in the sense wires,

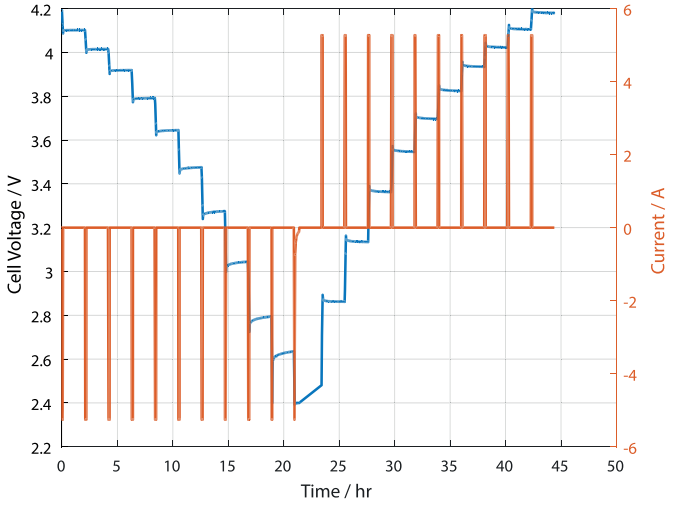

Fig. 7. Experimental test profile to find the OCV-SoC relationship of LIM5H cells.

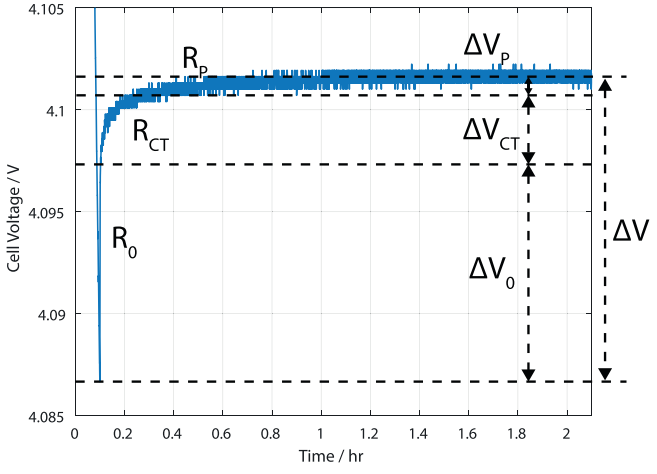

Fig. 8. The relaxation of the cell voltage for a LIM5H cell, after a 1C charge.

there is an immeasurable loss due to the connection.

However, when connected in a pack, this is not the case for the output, which will experience a voltage drop due to connections within the pack. Therefore, this is an input which is added to the multi-cell model and represents a constant addition to the resistance as per Eq. (3):

$$R_{Total} = R_{Cell} + R_{Connection} \tag{3}$$

Fig. 9 shows R_{DCIR} for the LIM5H cell using the method presented above, using OCV for V_{rest} to find the voltage drop. This is ideal, as it is fast and is the inverse method for how it is implemented in the model.

It can be seen that the measured impedance to charging is different from the impedance to discharging, also observed and modelled in [7]. The impedance changes across the range of SoC, and so charging and discharging impedance will be implemented separately in the model using two lookup tables based on the experimental result.

2.1.1.4. Temperature. . The results presented thus far have all been performed in tests within an environmental chamber at 25°C. Observations from real battery systems such as WESS suggest that there is often significant non-uniformity in temperature between cells in large-scale battery packs, as they are not in a closely controlled environment, despite the use of Heating, Ventilation and Air Conditioning (HVAC) systems. Therefore, it is helpful for a model to have temperature as an input, to be able to model the effects of changing temperature.

Some have observed that a reduction in temperature results in a reduction in cell voltage [25]. A test of 10 LIM5H cells at rest between 40°C and -10°C, with 2 h at each temperature at 50 % SoC showed no change in the Open Circuit Voltage. However, the impedance was shown to change. A short impedance test (350 ms pulse charge, 1C current) was used to minimise heating from the test. Considering Fig. 8, this 350 ms test finds a value for R_0.

It can be seen that the impedance trend is inversely proportional to temperature, which can be approximated with a linear approach as per Eq. (4). Some outliers can be seen in the data in Fig. 10, likely due to practical disturbances in the test, such as the environmental chamber door being erroneously opened.

$$R_T = (25 - T)^{*}0.0075R_{25} \tag{4}$$

where R_T is the resistance at T°C and R_{25} is the resistance at 25°C.

This is the purely ohmic impedance R_0, and assumes that $R_0 \propto R_{DCIR}$ for implementing it in the model. This method was chosen as the test is very short, so only a small amount of energy flows in or out of the battery, meaning the total heat generation from I^2R losses is very small. This in turn means that the cell temperature is as close to the environment temperature as possible. Later work involves improved modelling of temperature, but this is sufficient for general validation of the model and should indicate the effect of temperature on a battery, although it may not provide absolute values.

2.1.1.5. Coulombic efficiency. . Batteries do not have a perfect Coulombic Efficiency (CE), where CE is defined in Eq. (5) as:

$$CE = \frac{\int_{t_{ch,start}}^{t_{ch,end}} I \ dt}{\int_{t_{dch,start}}^{t_{dch,end}} I \ dt} \tag{5}$$

(adapted from [26]) This can be caused through the consumption of lithium or electrolyte and generally by side reactions in the cell during a cycle [26,27].

This will be calculated and implemented as an efficiency in the model, with half the efficiency factor applied during both charge and discharge, providing the correct overall CE. In reality, it is likely that there is differing CE during the charge and discharge phase [26], however, this would be very dependent on the chemistry as well as the age of the battery. Due to the fact that <1 CE is due to side reactions or lithium consumption, CE can be a factor which indicates degradation [28]. CE will be calculated using coulomb-counting from the capacity test with Eq. (5).

2.1.1.6. Degradation. In order to simulate the change in capacity with cycling, the model includes a factor for degradation based on the charge throughput for each cell, similar to the model described in [29–31]. The degradation factor is calculated based on the expected number of full cycles the cell will throughput before degrading to a specific proportion

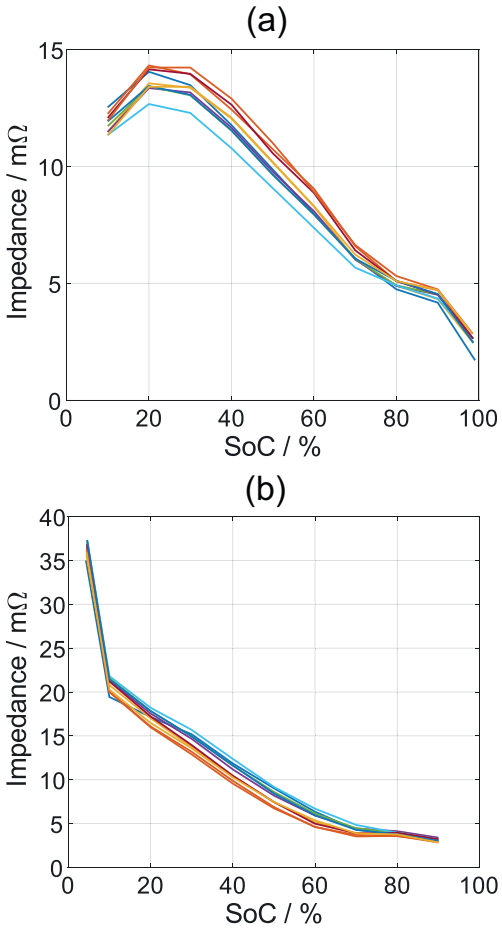

Fig. 9. R_{DCIR} of 10 LIM5H cells.

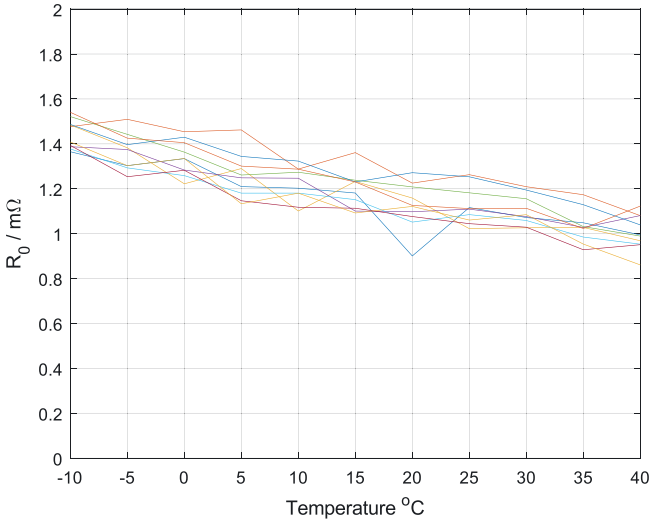

Fig. 10. R_0 vs temperature for a sample of 10 LIM5H Cells.

of its original capacity. Generally, a cell datasheet will state the number of cycles before reaching a given SoH. Eq. (6) shows the relationship implemented in the model, where the cell capacity reduces as a factor of energy throughput.

$$C_t = C_{t-1} - \Delta Q^* k, \tag{6}$$

where k is the degradation factor.

This is useful in the model as it should highlight whether some cells have a higher capacity throughput and are therefore degrading faster than others.

2.1.2. Cell model results

To validate the results for the single cell model, the model (shown in Simulink in Fig. 6) was parameterised using the experimental data from one of the LIM5H cells.

Three cycles were then performed on both the model and the physical cell at 2.5A, 5A and 7.5A (0.5C, 1C, 1.5C), so the results could be directly compared as shown below (Table 2).

Fig. 11 shows that the voltage profiles closely match, with only a small discrepancy. As expected, the dynamic behaviour is not exactly correct, as at the change from charge to discharge, the voltage jumps instantaneously, whereas the experimental result shows the change as somewhat damped due to the relaxation of the cell which is not modelled. This is more clear in Fig. 12.

The capacity of the pack shows a very accurate result, with a very small error. When considering the energy in the pack, this is slightly less accurate - likely due to the voltage not matching exactly due to the assumptions made in the impedance model.

2.2. Pack model

This section considers using the cell model to produce the proposed model of a large battery pack. Initially a model with just series connections is produced (3 s), then a model with just parallel connections (3p). These are then combined to give the full pack model (3s3p). Breaking the model down in this way allows better understanding and verification of the overall pack model.

Each of the three models is verified experimentally using data parameterised from the LIM5H cells. The packs were cycled using the MACCOR S4000. To measure the current in parallel connections, an LEM LTS 15NP current sensor was used, which has an accuracy of 0.2 %. These were connected to the MACCOR's 16-bit analogue inputs, each giving 0.0003 V resolution and a worst accuracy of 0.02 % (0.004 V). Using 3 primary turns on the current sensor, this gives a range of ±16A and therefore an accuracy of 32 mA at a resolution of 2 mA.

The experimental procedure used to validate the model is shown in Table 3.

This consists of four cycles, a single cycle as to reach thermal equilibrium and three test cycles, each at different C-rates to verify how accurately the model estimated the available capacity under conditions (which should result in differing capacities). Here, only constant current cycles are used, where a constant voltage cycle maybe used as an alternative. This was chosen to minimise the risk of a single cell becoming in an over-voltage state during a constant voltage charge.

Table 2
Summary of results comparing the model and experimental constant current capacity for a single LIM5H cell across 3 cycles at 0.5C, 1C and 1.5C.

	Mean model result	Mean experimental result	Mean model error	Error standard deviation
Discharge capacity/Ah	4.818	4.821	0.0035	0.0177
Charge capacity/Ah	4.804	4.794	−0.0099	0.0230
Discharge energy/Wh	17.111	17.161	0.0499	0.0288
Charge energy/Wh	17.474	17.361	−0.1132	0.1571

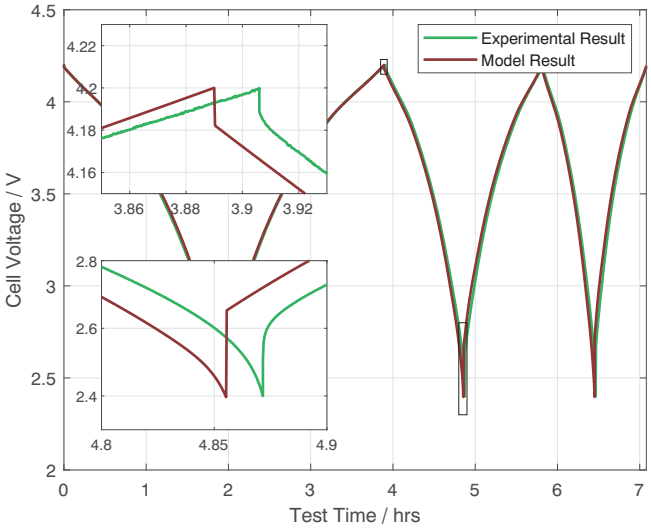

Fig. 11. Model vs experimental results for a single LIM5H cell.

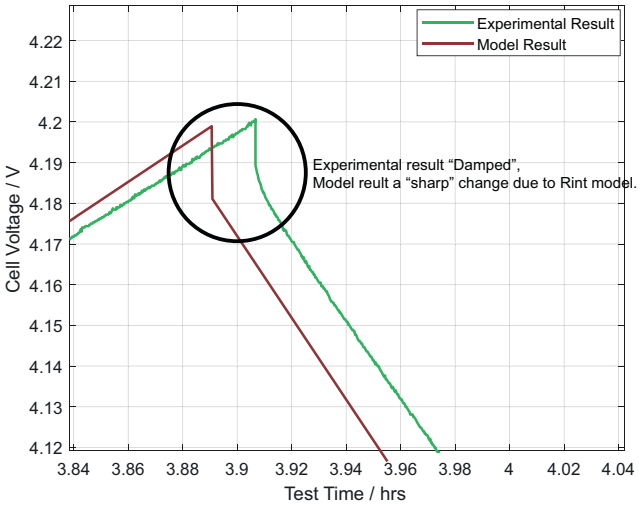

Fig. 12. Model vs experimental results for a single LIM5H cell, zoomed to the start of the 1C charge to highlight the different curve shape.

2.2.1. Series model

In the series model, the voltage and impedance of each cell are summed to produce the overall battery pack voltage. Three cells are modelled as shown in the diagram below. The cell models are labelled A-C and the cells which the model represents are labelled *1-n* (represented in italics), where n is the number of cells in the string. The cells are ranked strongest to weakest by capacity, with *cell 1* being the weakest and *cell n* being the strongest.

This results in Cell B being a model of the average capacity of *cell 2* to *cell n-1*, with the voltage being the number of *cells* in Cell B multiplied by the average cell voltage. Then summing the voltage of Cells A, B & C gives the overall pack voltage, shown by Eqs. (7) and (8).

$$V_A = V_1, \quad V_B = V_2 + \ldots + V_{n-1}, \quad V_C = V_n \tag{7}$$

$$V_{pack} = V_A + V_B + V_C \tag{8}$$

To compare the model with an experimental result, 3 LIM5H cells

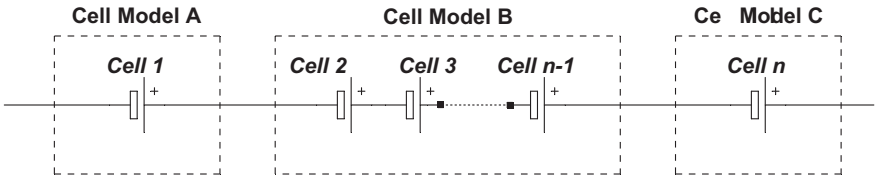

Fig. 13. Configuration of the cells in the cell models for a pack with series connections.

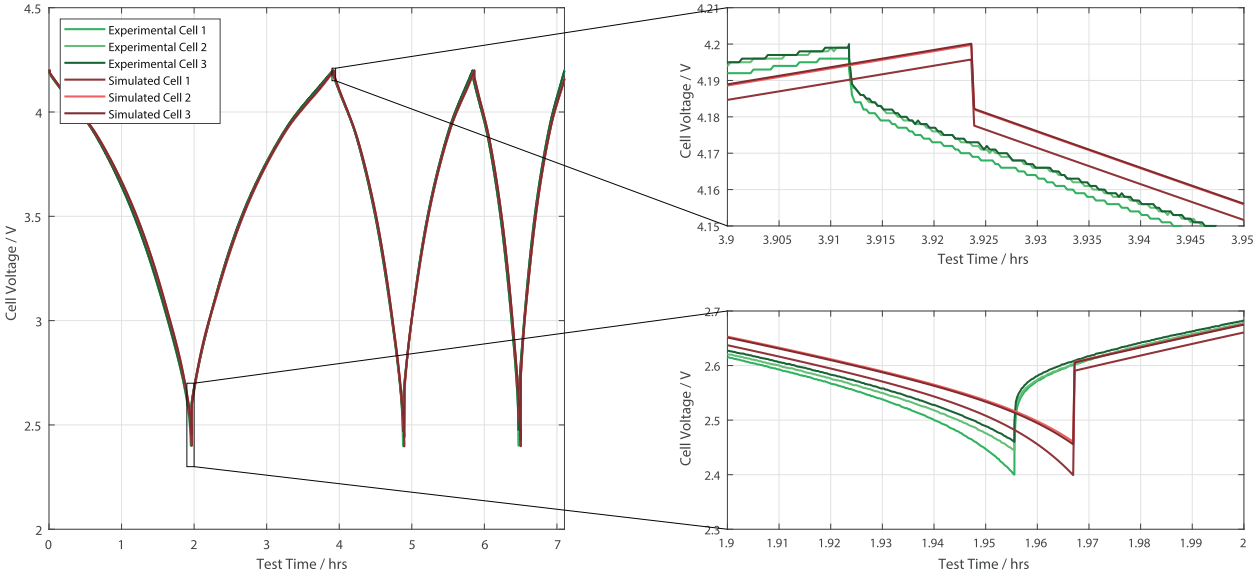

Fig. 14. Model vs experimental results for a 3 LIM5H cells connected in series.

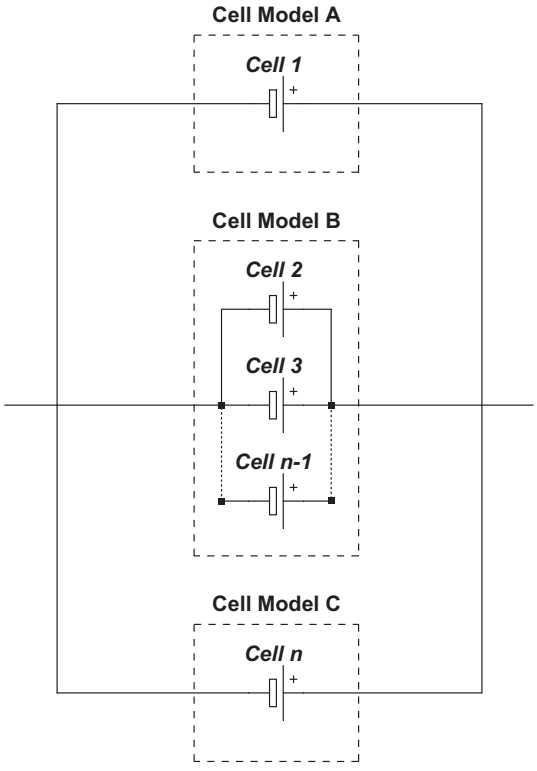

Fig. 15. Configuration of the cells in the cell models for a pack with parallel connections.

were used and 3 Constant Current (CC) cycles were performed as per the procedure in Table 3. The aim is to show that the voltages are different between cells during the cycles, which is reflected both experimentally and using the model in a simulation. The model parameters were found using the experimental data for the 3 cells used. The results are shown in Fig. 14.

It is clear from the figure that the voltage tracks as accurately as with the single cell model, and the error is in the same order of magnitude as with the single cell test.

2.2.2. Parallel model

The parallel model is modelled similarly to the series model as shown in the diagram in Fig. 15.

For Fig. 15, again the cells are ranked strongest to weakest by capacity, with *cell 1* being the weakest and *cell n* being the strongest. To identify parameters for cell model B, the capacity 'C' for all *cells* is summed as per Eq. (9), and impedance is calculated using the equation shown in 10:

$$C_A = C_1, \quad C_B = C_2 + \ldots + C_{n-1}, \quad C_C = C_n \tag{9}$$

$$R_A = R_1, \quad \frac{1}{R_B} = \frac{1}{R_2} + \ldots + \frac{1}{R_{n-1}}, \quad R_C = R_n \tag{10}$$

These are both straightforward, however, the voltage is constant between the cells. Given the same current, the cells would reach different voltages. In reality, different current flows through each cell due to different impedances and SoCs. For the model, a SimScape model was produced to calculate the current in each cell. Each cell consists of a voltage source and a resistor, which have values that are the cell voltage and cell impedance. These are connected in parallel as shown in the figure below (Fig. 16).

Again, to compare the model with an experimental result, 3 LIM5H

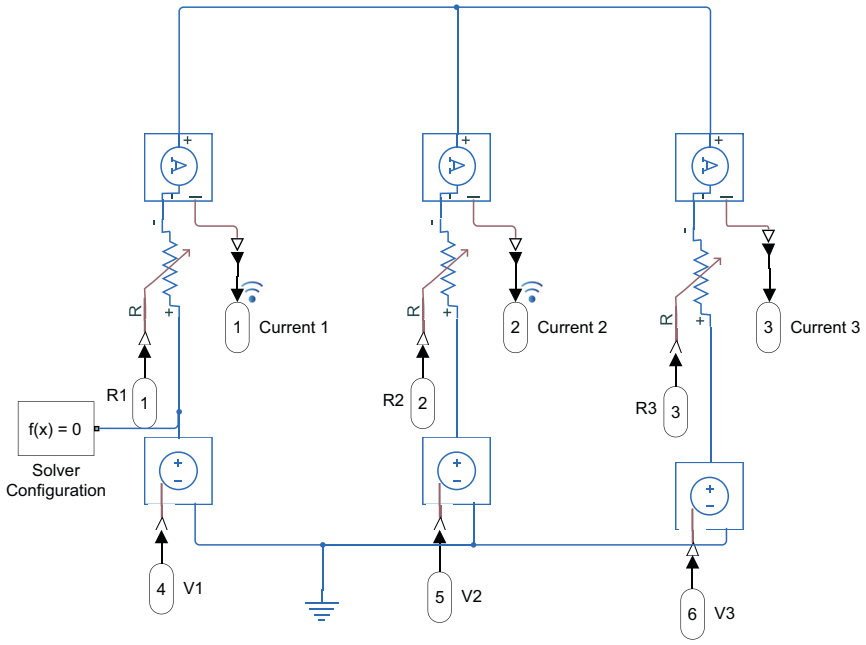

Fig. 16. Calculation of the current in each cell to ensure constant voltage using Simscape in Simulink.

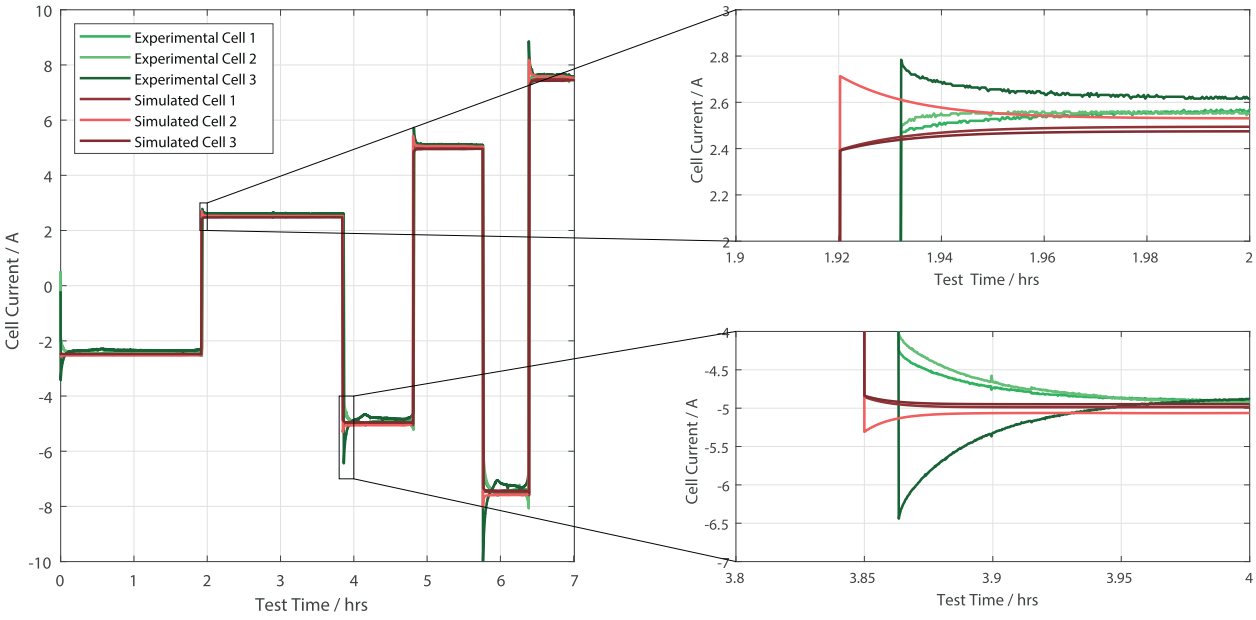

Fig. 17. Model vs experimental results for a 3 LIM5H cells connected in parallel showing the cell currents.

cells were used and 3 CC cycles were performed as per the procedure in Table 3. The model parameters were identified using the experimental data for the 3 cells used. It is expected that the voltage will be the same between cells and the current will vary between them, as this experiment will demonstrate. The current profile for each cell is shown in Fig. 17.

It can be seen in Fig. 17 that during a change in current, there is initially a large discrepancy in the current between the cells before it settles. In the model, this should show the cell which is working the 'hardest', or the cell that has the most current throughput and therefore will most likely see the most degradation. There is a larger current change seen in the experimental results than in the simulation. It is expected that this is due to a slightly higher connection impedance not accounted for in one cell compared to the others.

2.2.3. *Series and parallel combined model*

Combining the series and parallel models gives a model of the following architecture:

The cells are labelled similarly to the series and parallel model, with cells A-I being the 9 cell models which are computed. The *cells* which the model represents are labelled as *cell x/y* where *y* is the string number and *x* is the position in that string. *p* represents the number of parallel connected strings and *s* represents the number of cells in a series string.

To verify this model, a 3s3p pack was assembled and tested. Each *cell* had individual voltage and temperature measurements and each series string had a current measurement. This provides data points for all the cells being calculated by the model. By having accurate parameters for the 9 *cells*, these can be directly compared to the model results to observe where there are discrepancies between the model and reality, giving a

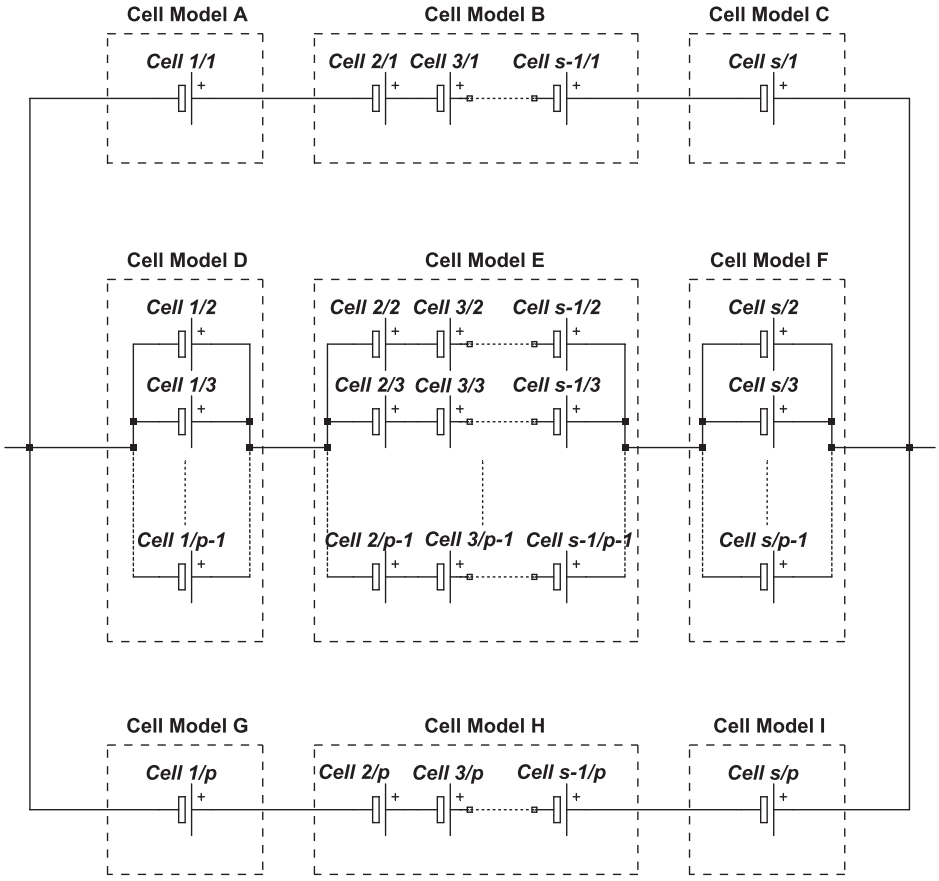

Fig. 18. Configuration of the cells in the cell models for a pack with series and parallel connections.

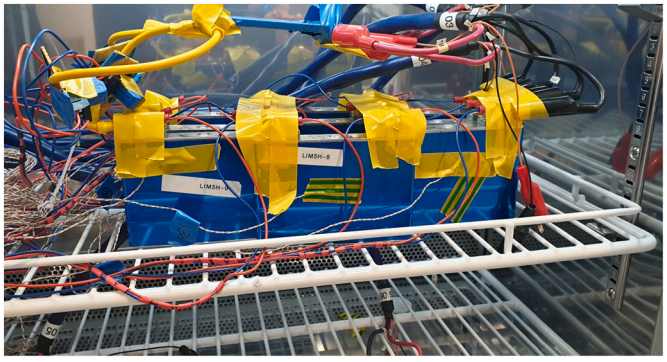

Fig. 19. An image of the experimental setup for LIM5H cells connected in a 3s3p configuration.

physical demonstration of the limitations. An image of the experimental setup is shown in Fig. 19.

It is expected that the model shows the same constant current capacity as the experimental pack, thereby verifying the assumptions made. A result within 1 % would be considered sufficient as it allows for the imbalance in SoC due to the accuracy of the MACCOR S4000. The results comparing the model with the experimental results are shown in Fig. 20 and Table 4.

This shows that for CC cycles of a 3s3p pack, the model is to within 1 % across a range of C-rates. It is expected that this accuracy would remain for a larger pack, assuming similarly good parameter identification. This notion will be verified in Section 4.

It can be seen that the current profiles are much better here than with the 3 parallel cells. This is likely due to a better connection which minimises the impedance differences between cells, and the same connection impedance would have less of an impact as there is greater impedance in each string with 3 cells in series.

3. Parameter identification

Section 2.1.1 discusses methods for identifying the parameters of the individual cells. This section considers how to 'scale up' the model, using a small sample of cells to estimate how a larger pack would behave by producing a sample with the same distribution. This new distribution can be used to populate the model in Fig. 18.

3.1. Variance

There is a difference between the capacity and impedance of each cell, considered as the variance. The following plot shows the capacity and impedance of each of the 10 cells.

As can be seen, there is little correlation between capacity and impedance, which agrees with other studies [32] - particularly with new cells.

Considering just the capacity and applying a normal distribution for the sample produces the distribution shown in Fig. 22.

This distribution can be used to produce a new dataset of any number of cells which matches the distribution. It is expected that the larger the dataset, the greater the chance the sample set includes outlier results.

For the impedance, it is not quite so straightforward as the impedance used in the model changes with SoC. Looking back at Fig. 9, as impedance increases, so does the difference in the impedance, suggesting that a multiplication factor would be ideal to define the variance between cells. This is done by taking the mean impedance at 50 % and multiplying to increase or decrease the impedance by the factor based on

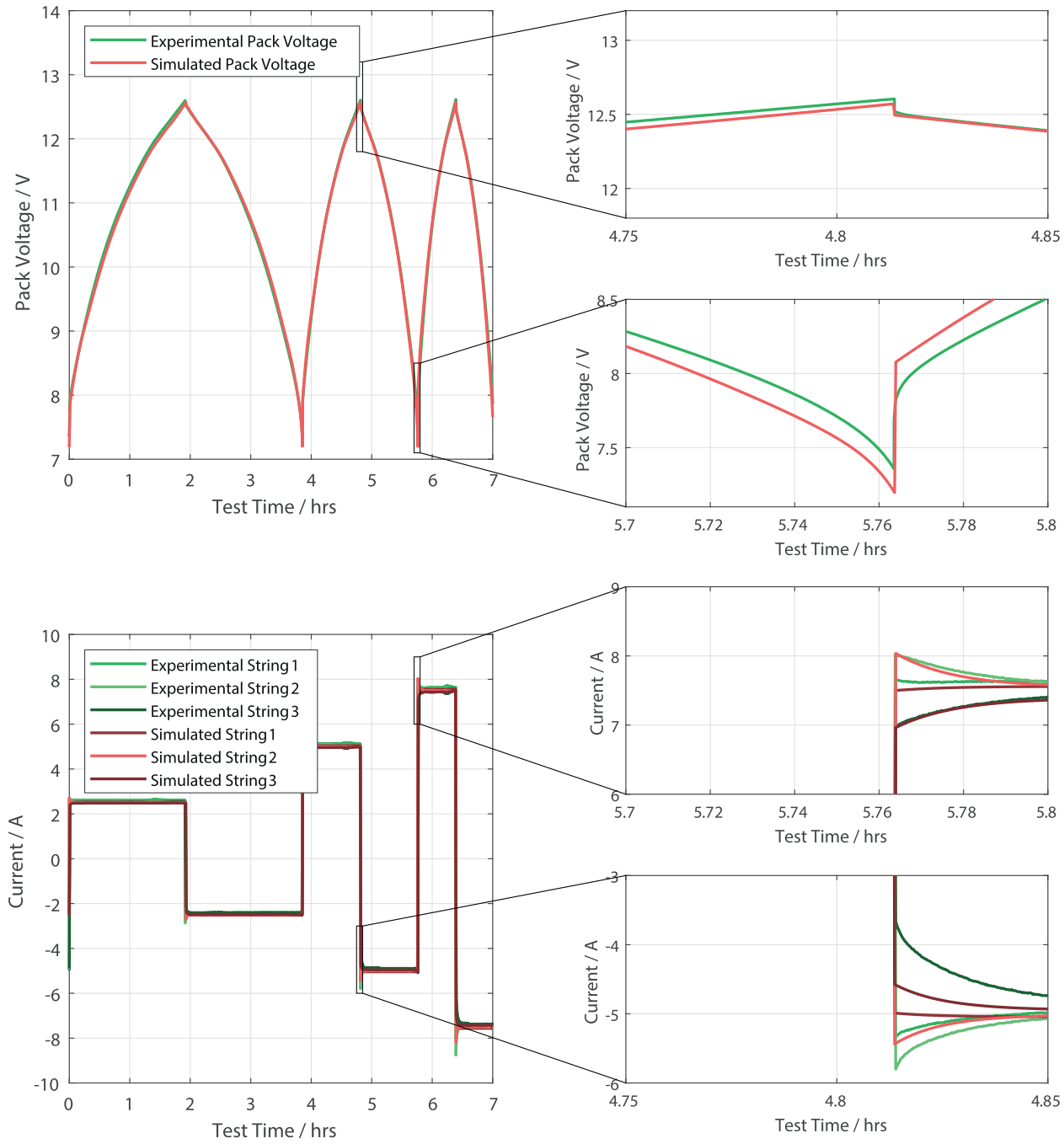

Fig. 20. Test profile showing the cell voltages in the model and the cell voltages from the experimental data.

the variance, as per Eq. (11), and is shown in Fig. 23.

$$R_x = R_{mean}{}^{*} k_x \tag{11}$$

where k_x is the variance factor for cell x and R_x is the impedance for cell x.

Using the discussed distribution of capacity and impedance, a sample of any number of cells can be produced which match the distribution.

3.2. Model population

To populate the model in Fig. 18 where there are >9 cells, it must be decided which cells are represented by which cell models.

In terms of individual cells, it has been shown in Fig. 21 that there is no correlation between capacity and impedance of a cell, so these values are distributed randomly among the sample of cells, except for the strongest and weakest cells. To consider the worst case scenario, the highest impedance cell can be given the lowest capacity for the weakest cell and the lowest impedance cell is given the highest capacity for the strongest cell. The cells are then distributed randomly into the pack, other than the strongest and weakest cells, which should be in different strings. If the worst case scenario is not being considered, then the cells are ranked by capacity to determine the weakest and strongest. The string containing the weakest cell is represented by cells A-C. Cell A represents the weakest cell in the string, cell C represents the strongest cell in the string and cell B represents a model of the remaining cells in the string. Similarly, the string containing the strongest cell is represented by cells G-I. Cell G represents the weakest cell in the string, cell I represents the strongest cell in the string and cell H represents a model of

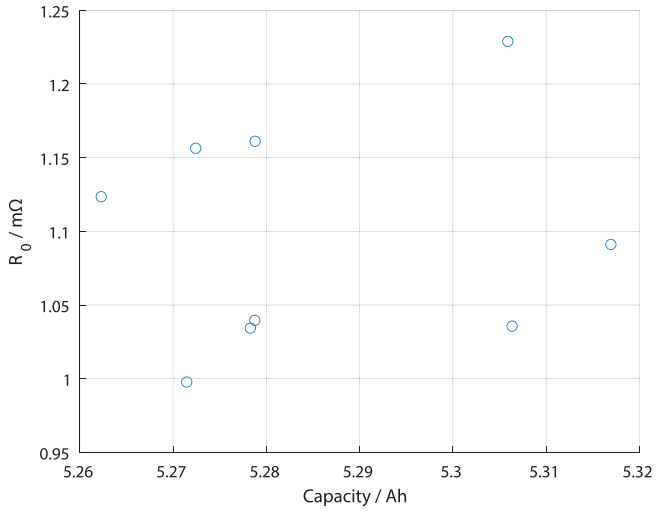

Fig. 21. R vs Capacity for a sample of 10 LIM5H Cells.

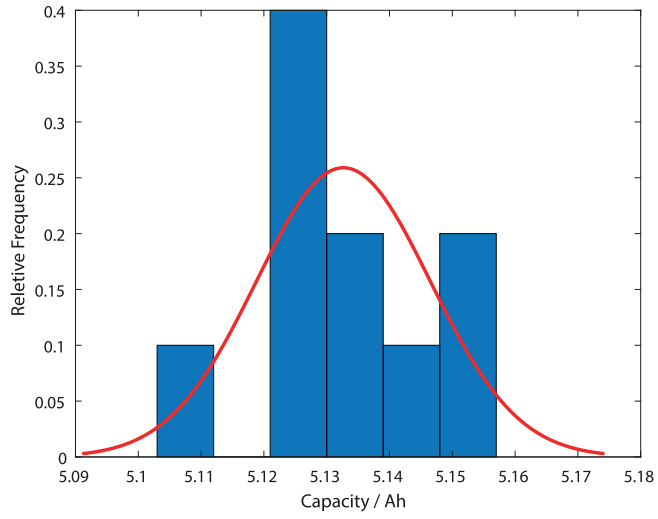

Fig. 22. Histogram with normal distribution showing distribution of capacities for sample of 10 LIM5H cells.

the remaining cells in the string. Finally, for the remaining strings, all weakest cells in each string are represented by a model in Cell D, all strongest cells in each string are represented by a model in Cell F and all remaining cells are represented by a model in cell E. This should give the metric for cell voltage imbalance and an indication of the currents flowing between the strings. This process is outlined in the flowchart and diagram in Figs. 24 and 25.

The previous section discussed and validated the model, where the number of cell models and number of cells is the same. For scale-up, a number of assumptions have been made. There is an element of randomness in identifying the parameters of a large model when creating a sample of cells from a distribution. This is because the MATLAB function used to produce the sample (RANDRAW), produces random values based on a distribution. Therefore, each time a set of samples is produced, it will be slightly different. Additionally, decisions have been made regarding which cells should be replaced by a single cell model and which ones should be grouped together into a single cell model. Therefore, to verify these assumptions, experimental work has been completed on a 12s4p pack, which will be discussed in the following section.

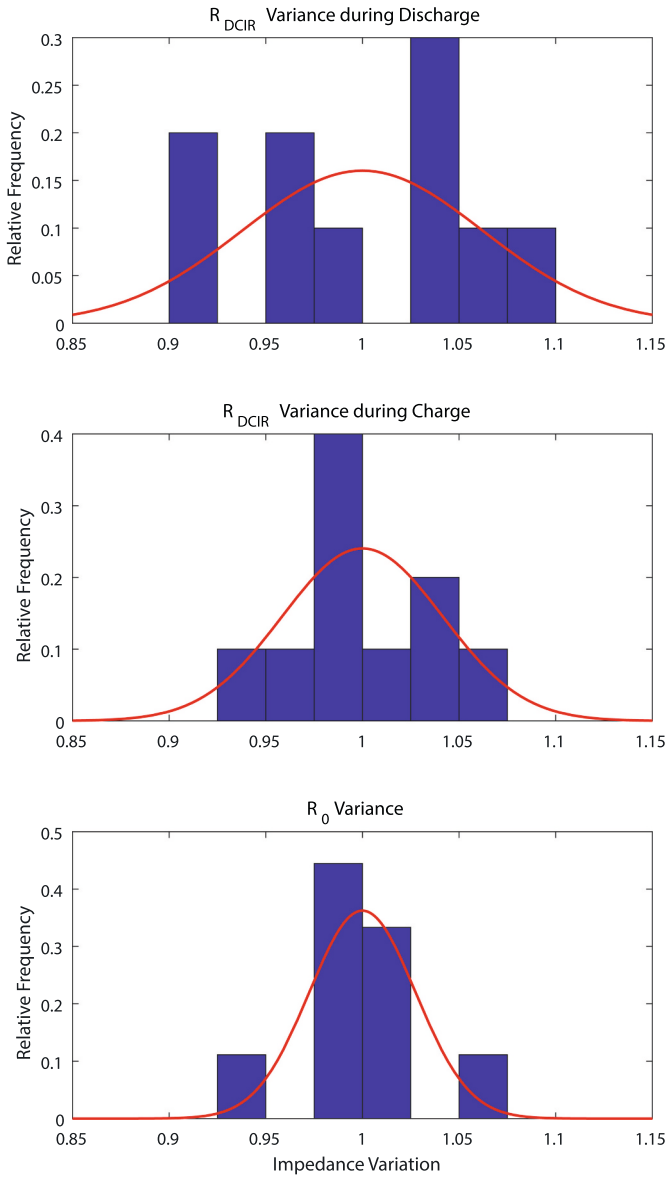

Fig. 23. Impedance variance from the mean impedance for a sample of 10 LIM5H cells, showing R_{DCIR} during charge and discharge.

4. Model evaluation

This study aims to produce a large battery pack model with a shorter simulation time than modelling every cell individually, but provides a more accurate model than modelling all cells as a single cell. This section will compare the modelling approach outlined in this paper to these two types of models. The same cell model will be used for each. For an experimental comparison, a 12s4p pack is used which is comprised of 4 Yuasa LIM50E modules connected in parallel. This configuration was chosen to verify the model population procedure outlined in Section 3.2 as there are >3 cells with series connections and >3 strings with parallel connections. This means that the model will be combining both parallel and series connections.

The cell model parameters were identified using the in-situ test method presented in [33], and the impedance and OCV relationships are shown in Figs. 26 & 27. A variance model was produced using the sample of 48 cells in the 12s4p pack giving the distribution of impedance and capacity shown in Fig. 28. This data was then used to populate the model using different methods, as will be discussed.

The tests performed experimentally and on the models were CC cycle

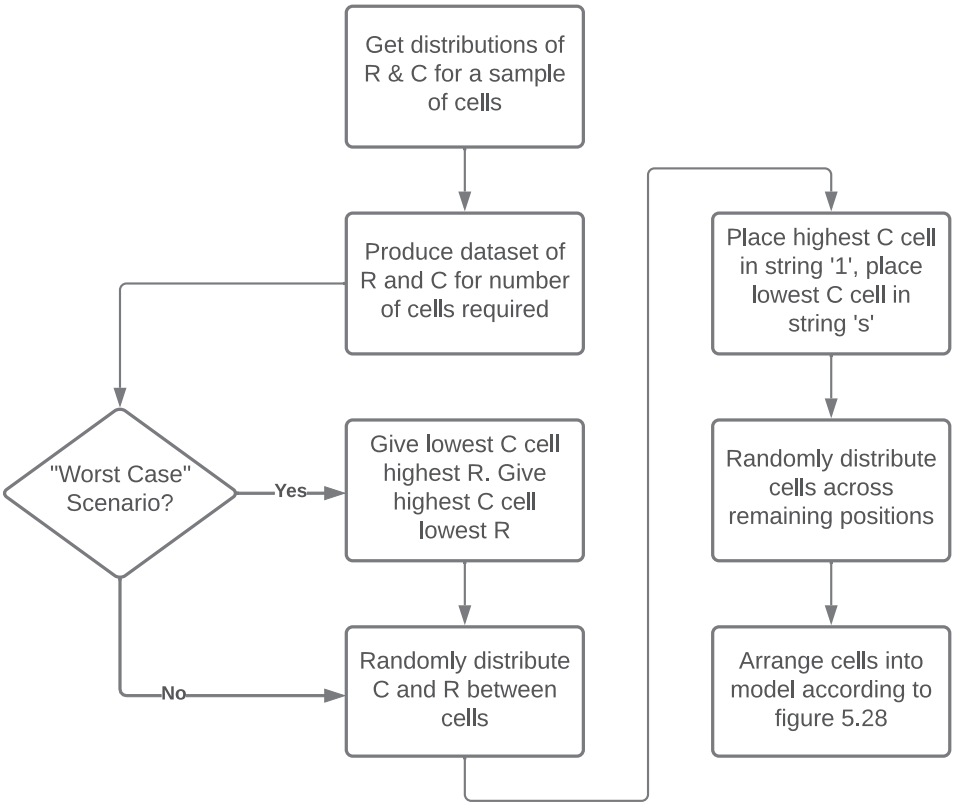

Fig. 24. Flowchart describing the method for producing a battery pack based on a distribution of Impedance (R) and Capacity (C).

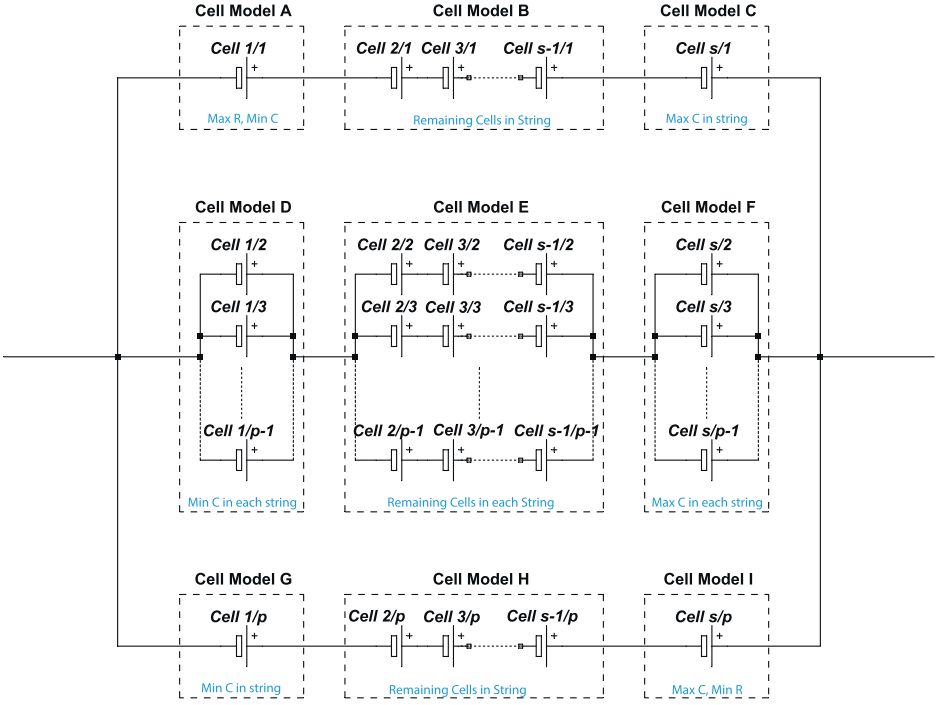

Fig. 25. Diagram showing where cells in a pack produced from the process in figure are located in the model.

tests at 0.25C, 0.5C, 0.75C and 1C. These C-rates were chosen as the maximum charge rate given by the manufacturer is 1C, and a range of C-rates were used to observe the model under different operating conditions. The test profile was as shown in Table 5.

The test was performed experimentally at the different C-rates and simulated under different scenarios. Two main experiments were performed:

- Comparison between models of varying numbers of cell models

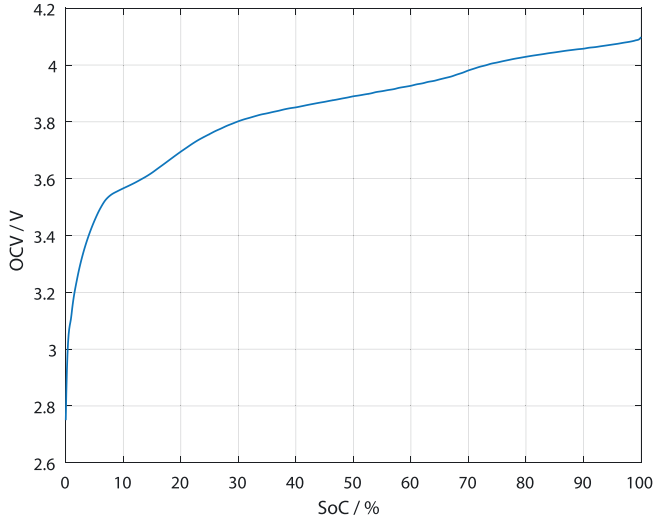

Fig. 26. OCV vs SOC relationship for LIM50E cells used to identify the parameters for the model.

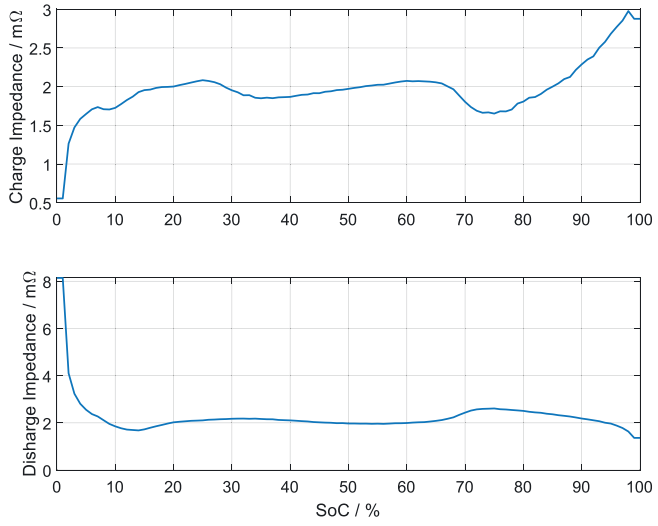

Fig. 27. Mean impedance relationship for LIM50E cells used to identify the parameters for the model.

- Comparison between using experimentally derived parameters and using parameters generated from a distribution.

4.1. Varying numbers of cell models

For a baseline, an All Cells Model (ACM) was simulated - a model consisting of a cell model representing each cell. The parameters used in the model were those which were experimentally measured. Additionally, a model consisting of a single cell model Single Cell Model (SCM) which represents the entire pack was also simulated, again using the parameters experimentally measured. These were then compared to the 9CM. Parameters were chosen using the weakest cell ranked as the cell with the lowest capacity and equally the strongest cell ranked as the cell with the highest capacity. The model was populated respecting the configuration of the parameters in the experimental pack. The results for the CC cycle tests at different C-rates found experimentally, and using these models are shown in Table 6. The average percentage error of each model compared to the experimental result is shown in Table 7, along with the standard deviation across C-rates.

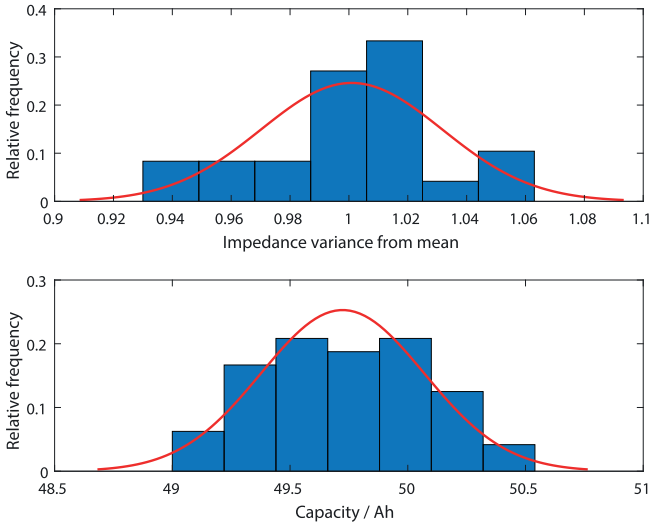

Fig. 28. Impedance and Capacity distributions for a sample of 48 LIM50E cells used to identify the parameters for the model.

Table 3
Test procedure for verification of the model.

Sequence	Limits	End condition
CC charge	I = 1C	Any cell ≥ Max V
CC discharge	I = 1C	Any cell ≤ Min V
CC charge	I = 0.5C	Any cell ≥ Max V
CC discharge	I = 0.5C	Any cell ≤ Min V
CC charge	I = 1C	Any cell ≥ Max V
CC discharge	I = 1C	Any cell ≤ Min V
CC charge	I = 1.5C	Any cell ≥ Max V
CC discharge	I = 1.5C	Any cell ≤ Min V

Table 4
Summary of results comparing the model and experimental results for a 3s3p pack made from LIM5H cells.

	Model capacity/ Ah	Experimental capacity/ Ah	Model error/ %
0.5C discharge	14.28	14.24	0.26
0.5C charge	14.21	14.24	−0.24
1C discharge	14.08	14.09	−0.02
1C charge	14.00	13.92	0.57
1.5C discharge	13.88	13.87	0.08
1.5C charge	13.79	13.78	0.11

Table 5
Test sequence for testing a 12s4p pack of LIM50E cells. The portion of the test sequence used for the results is shown in bold.

Sequence	Limits	End condition
CC charge	I = 1C	Any cell ≥ Max V
CC discharge	I = 1C	Any cell ≤ Min V
CC charge	I = Test C-rate	Any cell ≥ Max V
CC discharge	I = Test C-rate	Any cell ≤ Min V
CC charge	I = Test C-rate	Any cell ≥ Max V

It can be seen that the ACM performs identically to the proposed 9CM. These are not perfect, however, are within a 1 % tolerance, with different errors at different C-rates. The model correlates best at 1C, which is unsurprising, as the parameters were identified using tests at 1C. The errors are likely due to inconsistent temperatures between the different tests (future work considers this). The SCM is notably worse,

Table 6
Comparison for the capacity across a range of C-rates for the 3 different model types.

Capacity/Ah	0.25C	0.5C	0.75C	1C
Experimental	180.1	169.6	159.6	150.0
ACM	184.6	170.6	159.1	150.8
SCM	186.3	172.5	161.0	152.7
9CM	184.6	170.6	159.1	150.8

Table 7
Comparison of the error for simulations of the 3 different model types compared to the experimental results.

	Error	Std. Deviation
ACM	0.82 %	1.00 %
SCM	1.90 %	0.90 %
9CM	0.82 %	1.00 %

with approximately 2 % error on average.

Considering the simulation time, it can be seen in Table 8 that simulation of the ACM took 80s, whereas the proposed 9CM only took 4 s. For virtually the same result, this is a significant improvement.

4.2. Generating parameters from a distribution

The 9CM simulation result using experimental parameters can then be compared to using the variance relationship to identify the parameters for the model. The distribution shown in Fig. 28 was used to produce a sample of 48 cells. The sample was then used to populate the model for a "worst case" scenario according to the method outlined in 3.2, where the "weakest cell" has the lowest capacity and highest impedance. Additionally, the model was populated with impedance and capacity distributed randomly, with the weakest cell ranked by capacity as with the simulation of the 9CM in Table 6. The capacity for these is shown in Tables 9 and 10.

Using variance to produce a dataset produced a similar result, however, with a lower constant current capacity (2 %) than using the parameters found experimentally.

4.3. Discussion

The results show that modelling all cells in the 12s4p pack will give virtually the same capacity as the proposed model which considers nine cells in a 3s3p configuration when simulating cycles at a constant current different C-rates. With just a single cell model, the result is around 1 % worse across the range of C-rates.

Generating parameters from a distribution gives a similar error to using experimental parameters, however gives lower capacity estimations than were experimentally found. This is likely due to the distribution producing more outliers than are in the experimental pack. A reason for this could be due to manufacturer selection, where new cells are tested, and poorer performing cells removed.

One error is that at lower C-rates, the experimental capacity was found to be lower than the expected capacity from the simulations. It is expected that this is due to temperature, which was not compensated for as there is poor temperature sensing on the LIM50E modules, with only one measurement for all of the 12 cells in each module. At a lower C-rate, the cell will generate less heat over a given time period, meaning the cell temperature is lower, thereby reducing the impedance according to the relationship found in Section 2.1.1. Future work involves sensing temperature for each cell individually to be able to compensate for the temperature-related errors and producing a model to simulate changes in temperature.

Table 8
Comparison of test times for the 3 different model types for a 10 h experiment.

	Test time for 10 h simulation/s
Experimental	36,000.0
ACM	79.6
SCM	1.2
9CM	3.7

Table 9
Comparison for the capacity across a range of C-rates for the 9CM for different model population methods, where parameters are generated from the variance relationship.

Capacity/Ah	0.25C	0.5C	0.75C	1C
Experimental	180.1	169.6	159.6	150.0
Generated parameters Impedance/capacity distributed randomly	182.8	168.5	156.9	148.4
Generated parameters Pack configured as weakest cell has highest impedance	182.1	167.7	156	147.3

Table 10
Comparison of the error compared to the experimental result across a range of C-rates (shown in Table 9 for the 9CM for different model population methods, where parameters are generated from the variance relationship).

Capacity	Mean Error	Std. Dev
Generated parameters Impedance/capacity distributed randomly	−0.47 %	1.20 %
Generated parameters Pack configured as weakest cell has highest impedance	−1.03 %	1.29 %

5. Conclusions

In conclusion, the proposed model consisting of 9 cell models, has been shown to model a large battery with the same accuracy as modelling all cells, yet with a reduced simulation time comparable to that of simulating a single cell. At 1C, a 12s4p pack was experimentally found to have a capacity of 150 Ah and the proposed model estimated a capacity of 150.8 Ah - identical to modelling all cells. Modelling all cells however took 79.6 s, whereas the proposed model took just 3.7 s, showing its significantly improved computational efficiency. It has been shown that it is a viable option to model a sample of cells from a distribution to simulate the behaviour of a different sample of cells which follow the same distribution, as when generating parameters based on the distribution of a sample of cells, the proposed model gave a capacity of 148.4 Ah. These will enable fast modelling of large batteries to predict how they will behave under different conditions.

Future work involves using the model to investigate how different scenarios can affect a battery, for example, the optimal SoC to perform cell balancing at and determining a level of cell voltage imbalance that is safely acceptable. Finally, further experimentation using cell-level data from WESS will be used to evaluate the model at a larger scale, using the model to inform a real-time estimator.

CRediT authorship contribution statement

T L Fantham: Methodology, Experimental, Modelling, Formal analysis, Investigation, Writing – Original Draft.

D T Gladwin: Supervision, Conceptualization, Resources, Writing – Review & Editing.

Declaration of competing interest

The authors declare that they have no known competing financial interests or personal relationships that could have appeared to influence the work reported in this paper.

Data availability

Data will be made available on request.

Acknowledgements

The authors gratefully acknowledge support from the EPSRC via grant EP/L016818/1 which funds the Centre for Doctoral Training in Energy Storage and its Applications.

References

[1] T. Bruen, J. Marco, Modelling and experimental evaluation of parallel connected lithium ion cells for an electric vehicle battery system, J. Power Sources 310 (2016) 91–101, https://doi.org/10.1016/j.jpowsour.2016.01.001.
[2] D. Baek, Y. Chen, N. Chang, E. Macii, M. Poncino, Battery-aware electric truck delivery route exploration, Energies 13 (2020) 1–18, https://doi.org/10.3390/en13082096.
[3] T. Feehally, D. Gladwin, R. Todd, A. Forsyth, M. Foster, D. Strickland, D. Stone, Battery energy storage systems for the electricity grid: Uk research facilities, in: The 8th IET International Conference on Power Electronics, Machines and Drives (PEMD 2016), 2016, pp. 1–6, https://doi.org/10.1049/cp.2016.0257.
[4] F. Milano, Álvaro Ortega Manjavacas, Converter-interfaced Energy Storage Systems: Context, Modelling and Dynamic Analysis, Cambridge University Press, 2019, https://doi.org/10.1017/9781108363266.
[5] Neoen, Hornsdale power reserve — south australia's big battery, URL, https://hornsdalepowerreserve.com.au/.
[6] T.L. Fantham, D.T. Gladwin, Impact of cell balance on grid scale battery energy storage systems, Energy Rep. 6 (2020) 209–216, https://doi.org/10.1016/j.egyr.2020.03.026.
[7] M. Ye, X. Song, R. Xiong, F. Sun, A novel dynamic performance analysis and evaluation model of series-parallel connected battery pack for electric vehicles, IEEE Access 7 (2019) 14256–14265, https://doi.org/10.1109/ACCESS.2019.2892394.
[8] F. Baronti, R.D. Rienzo, N. Papazafiropulos, R. Roncella, R. Saletti, Investigation of series-parallel connections of multi-module batteries for electrified vehicles, in: 2014 IEEE International Electric Vehicle Conference, IEVC 2014, 2014, pp. 1–7, https://doi.org/10.1109/IEVC.2014.7056173. Distribution¡br/¿¡br/¿variance model.
[9] F. Chang, F. Roemer, M. Baumann, M. Lienkamp, Modelling and evaluation of battery packs with different numbers of paralleled cells, World Electr. Vehicle J. 9 (6) (2018), https://doi.org/10.3390/wevj9010008.
[10] S. Nejad, D.T. Gladwin, D.A. Stone, A systematic review of lumped-parameter equivalent circuit models for real-time estimation of lithium-ion battery states, J. Power Sources 316 (2016) 183–196, https://doi.org/10.1016/j.jpowsour.2016.03.042.
[11] X. Lai, Y. Zheng, T. Sun, A comparative study of different equivalent circuit models for estimating state-of-charge of lithium-ion batteries, Electrochim. Acta 259 (2018) 566–577, https://doi.org/10.1016/j.electacta.2017.10.153. Distribution ¡br/¿¡br/¿variance model.
[12] H. He, R. Xiong, J. Fan, Evaluation of lithium-ion battery equivalent circuit models for state of charge estimation by an experimental approach, Energies 4 (2011) 582–598, https://doi.org/10.3390/en4040582.
[13] R. Xiong, F. Sun, H. He, State-of-charge estimation of lithium-ion batteries in electric vehicles based on an adaptive extended kalman filter, Gaojishu Tongxin Chin. High Technol. Lett. 22 (2012) 198–204, https://doi.org/10.3772/j.issn.1002-0470.2012.02.014.
[14] S. Li, H. He, C. Su, P. Zhao, Data driven battery modeling and management method with aging phenomenon considered, Appl. Energy 275 (2020), 115340, https://doi.org/10.1016/j.apenergy. 2020.115340.
[15] M. Daowd, N. Omar, P. van den Bossche, J. van Mierlo, A review of passive and active battery balancing based on matlab/simulink, Int. Rev. Electric. Eng. 6 (2011) 2974–2989, helpful review of balancing mechanisms¡br/¿¡br/¿Lots of references.
[16] S. Wang, C. Fernandez, C. Yu, Y. Fan, W. Cao, D.I. Stroe, A novel charged state prediction method of the lithium ion battery packs based on the composite equivalent modeling and improved splice kalman filtering algorithm, J. Power Sources 471 (9) (2020), https://doi.org/10.1016/j.jpowsour.2020.228450.
[17] C. Burgos-Mellado, M.E. Orchard, M. Kazerani, R. Cárdenas, D. Sáez, Particle-filtering-based estimation of maximum available power state in lithium-ion batteries, Applied Energy 161 (2016) 349–363, https://doi.org/10.1016/j.apenergy.2015.09.092, impedance changes with c-rate¡br/¿¡br/¿rint model used.
[18] X. Zeng, M. Li, D.A. El-Hady, W. Alshitari, A.S. Al-Bogami, J. Lu, K. Amine, Commercialization of lithium battery technologies for electric vehicles, Adv. Energy Mater. 9 (2019) 1–25, https://doi.org/10.1002/aenm.201900161.
[19] C. Pastor-Fernández, W. Widanage, G. Chouchelamane, J. Marco, A soh diagnosis and prognosis method to identify and quantify degradation modes in li-ion batteries using the ic/dv technique, in: 6th Hybrid and Electric Vehicles Conference (HEVC 2016), 2017, pp. 1–6, https://doi.org/10.1049/cp.2016.0966.
[20] A. Barai, K. Uddin, W.D. Widanage, A. McGordon, P. Jennings, A study of the influence of measurement timescale on internal resistance characterisation methodologies for lithium-ion cells, Sci. Rep. 8 (2018) 1–13, https://doi.org/10.1038/s41598-017-18424-5.
[22] H. He, R. Xiong, H. Guo, S. Li, Comparison study on the battery models used for the energy management of batteries in electric vehicles, Energy Convers. Manag. 64 (2012) 113–121, https://doi.org/10.1016/j.enconman.2012.04.014.
[23] V.L. Pham, V.T. Duong, W. Choi, A low cost and fast cell-to-cell balancing circuit for lithium-ion battery strings, Electronics (Switzerland) 9 (2020) 248, https://doi.org/10.3390/electronics9020248, uses same technique as me for OCV and IR.
[24] W. Waag, S. Käbitz, D.U. Sauer, Experimental investigation of the lithium-ion battery impedance characteristic at various conditions and aging states and its influence on the application, Appl. Energy 102 (2013) 885–897, https://doi.org/10.1016/j.apenergy.2012.09.030.
[25] A. Purwadi, A. Rizqiawan, A. Kevin, N. Heryana, State of charge estimation method for lithium battery using combination of coulomb counting and adaptive system with considering the effect of temperature, in: Proceedings - ICPERE 2014: 2nd IEEE Conference on Power Engineering and Renewable Energy 2014, 2014, pp. 91–95, https://doi.org/10.1109/ICPERE.2014.7067233. Good block diagram of model.
[26] X. Ni, Y. He, H. Wang, Expanding the metrology of coulombic efficiency using neutron depth profiling, Radiat. Eff. Defects Solids 175 (2020) 356–366, https://doi.org/10.1080/10420150.2019.1701467.
[27] J.C. Burns, G. Jain, A.J. Smith, K.W. Eberman, E. Scott, J.P. Gardner, J.R. Dahn, Evaluation of effects of additives in wound li-ion cells through high precision coulometry, J. Electrochem. Soc. 158 (2011) A255, https://doi.org/10.1149/1.3531997.
[28] F. Yang, D. Wang, Y. Zhao, K.L. Tsui, S.J. Bae, A study of the relationship between coulombic efficiency and capacity degradation of commercial lithium-ion batteries, Energy 145 (2018) 486–495, https://doi.org/10.1016/j.energy.2017.12.144.
[29] E. Namor, D. Torregrossa, F. Sossan, R. Cherkaoui, M. Paolone, Assessment of battery ageing and implementation of an ageing aware control strategy for a load leveling application of a lithium titanate battery energy storage system, 2016 IEEE 17th workshop on control and modeling for power electronics, COMPEL 2016 (2016) 1–6, https://doi.org/10.1109/COMPEL.2016. 7556779.
[30] X. Tan, Y. Wu, D.H. Tsang, A stochastic shortest path framework for quantifying the value and lifetime of battery energy storage under dynamic pricing, IEEE Trans. Smart Grid 8 (2017) 769–778, https://doi.org/10.1109/TSG.2015.2478599.
[31] J.D. Bishop, C.J. Axon, D. Bonilla, M. Tran, D. Banister, M.D. McCulloch, Evaluating the impact of v2g services on the degradation of batteries in phev and ev, Appl. Energy 111 (2013) 206–218, https://doi.org/10.1016/j.apenergy.2013.04.094.
[32] S.F. Schuster, M.J. Brand, C. Campestrini, M. Gleissenberger, A. Jossen, Correlation between capacity and impedance of lithium-ion cells during calendar and cycle life, J. Power Sources 305 (2016) 191–199, https://doi.org/10.1016/j.jpowsour.2015.11.096.
[33] T.L. Fantham, D.T. Gladwin, In-situ Parameter Identification of Cells in Grid-connected Batteries Vol. 2021-October, IEEE Computer Society, 2021, https://doi.org/10.1109/IECON48115.2021.9589240.